ChemComm

RSC Publishing

COMMUNICATION

View Article Online
View Journal | View Issue

Cite this: *Chem. Commun.*, 2013, **49**, 11788

Received 7th September 2013,
Accepted 24th October 2013

DOI: 10.1039/c3cc46863a

www.rsc.org/chemcomm

Stoichiometry-controlled FeP nanoparticles synthesized from a single source precursor†

Cornelia Hunger,[a] Wilfried-Solo Ojo,[b] Susanne Bauer,[a] Shu Xu,[b] Manfred Zabel,[a] Bruno Chaudret,[b] Lise-Marie Lacroix,[b] Manfred Scheer,*[a] Céline Nayral*[b] and Fabien Delpech*[b]

Phase-pure FeP nanoparticles (NPs) have been synthesized through low temperature thermolysis of the single source precursor $[(CO)_4Fe(PH_3)]$. Examination of the mechanism demonstrates the central role of the labile CO ligands and the weak P–H bonds to yield stoichiometry controlled FeP materials.

Iron phosphides belong to a fascinating class of low-cost materials, exhibiting different properties depending on their phase (Fe_3P, Fe_2P, FeP, FeP_2 and FeP_4), and thus targeting a wide scope of applications (ferromagnetism, magnetoresistance, magneto-calorific effects, catalysis, and batteries).[1–4] However, the synthesis of size- and stoichiometry-controlled iron phosphide nanoparticles (NPs) still remains highly challenging. This is in particular the case for FeP,[2] which is of high interest for energy applications such as electrocatalysis for hydrogen production[3] or electrodes of Li-ion batteries.[4] As recently reviewed by Carenco *et al.*, the synthetic routes can be classified according to the phosphorus source: *in situ or ex situ*-generated phosphine (PH_3), elemental phosphorus, tris(trimethylsilyl)phosphine ($P(SiMe_3)_3$) and trioctylphosphine (TOP).[5] Considered as more convenient, less expensive and safer than other sources, trioctylphosphine (TOP) has been privileged during the last decade.[1,2,5–11] However, the use of TOP goes along with certain limitations in terms of phase control or mechanistic understanding.[3] The lack of reactivity of TOP indeed requires to work at very high temperature (>300 °C) to break the strong P–C bonds. These harsh conditions facilitate atomic recombination and thus, the phase control will be essentially based on sophisticated procedures involving slow syringe injections, multistep heating ramp or solutions containing partially decomposed precursors.[5] As successful examples, Brock *et al.* and Hyeon *et al.* reported the challenging pure-phase formation of Fe_2P[2,10] and FeP[2] NPs by transformation of Fe nanoparticles in the presence of TOP. Concerning the mechanistic aspects, the complexity of these procedures (continuous delivery of the precursors[10] and multistep heating ramps[2]) and the high temperature make the rationalisation difficult from the chemical viewpoint.[5]

As an alternative, a single source approach using organometallic precursors may be considered as an elegant and pertinent alternative to control the phase and the purity of nanomaterials.[12,13] Indeed, the predetermined stoichiometry is anticipated to form a target phase and decomposition is expected to be controllable (thanks to adjustable metal–ligand interactions) and to occur in narrower and lower temperature ranges.[14] However, the results reported in the literature are often disappointing in terms of phase control. In the sole examples of nanoscaled iron phosphide NPs, the use of the single source precursors $Fe(CO)_4[PPh_2CH_2CH_2Si(OMe)_3]$[15] and $[H_2Fe_3(CO)_9P^tBu]$[16] required high temperature (>310 °C) to achieve decomposition and failed in establishing a correlation between precursor stoichiometry and the final product. Both complexes yielded Fe_2P nanomaterials instead of the expected FeP and Fe_3P NPs, presumably because of interactions between the precursor and the stabilizing agents during the synthesis.[14]

Thus, this brief overview shows the limits of the currently developed methods in terms of phase control or mechanistic understanding and suggests that the development of precursors designed for this specific objective is necessary to take up these challenges. We identified $[(CO)_4Fe(PH_3)]$[17,18] (**1**) as a valuable candidate as a single source precursor for FeP nanoparticles, meeting the requirements of the weakness of P–H bonds (compared for example to P–C ones) and the lability of the CO ligands,[19] as evidenced by the use of the related binuclear complex $FeMn(CO)_8(\mu\text{-}PH_2)$ for preparing $Fe_{2-x}Mn_xP$ NPs.[20] In addition, the relevance of this type of complex for the preparation of various clusters including phosphorus naked atoms has also been recently evidenced.[21] In the present study, we have successfully designed a reliable and straightforward strategy for the synthesis of **1** and we report the photochemical and the chemical behaviours of this complex which led, first, to an unprecedented isolated intermediate and then, to FeP NPs with controlled size and stoichiometry.

[a] *Institut für Anorganische Chemie, Universität Regensburg, Regensburg D-93053, Germany. E-mail: manfred.scheer@chemie.uni-regensburg.de*

[b] *Université de Toulouse; INSA, UPS, CNRS; LPCNO (Laboratoire de Physique et Chimie des Nano-Objets), 135 avenue de Rangueil, F-31077 Toulouse, France. E-mail: fabien.delpech@insa-toulouse.fr, celine.nayral@insa-toulouse.fr*

† Electronic supplementary information (ESI) available: Synthetic procedures, temporal evolution of the FT-IR spectrum during the synthesis of FeP nanoparticles, the Mössbauer spectrum, XRD patterns, HRTEM pictures and selected area diffraction patterns. CCDC 959696. For ESI and crystallographic data in CIF or other electronic format see DOI: 10.1039/c3cc46863a

Taking advantage of our expertise in metal pnictides,[21] we have recently reported the synthesis of $[(CO)_4W(PH_3)_2]$ by the "one-pot" reaction of $[(CO)_4W(nbd)]$ (nbd = norbornadiene) with $P(SiMe_3)_3$ and subsequent methanolysis of the reaction mixture.[22] The advantages of this synthetic route are good yields and that use of PH_3 is avoided. We have successfully transferred this concept to the formation of **1** (see ESI† for X-ray structure) which was obtained in excellent yields using the same route as that previously described for $[(CO)_4W(PH_3)_2]$ (eqn (1)).[22]

$$[Fe(CO_5)] + P(SiMe_3)_3 \xrightarrow[-CO]{h\nu/THF} \xrightarrow[-3MeOSiMe_3]{+3MeOH} [(CO)_4Fe(PH_3)] \quad (1)$$

FeP nanoparticles were prepared *via* thermolysis of the single source mononuclear complex **1** at 150 °C. Remarkably, and in contrast to most of the previous synthetic routes, these particles were obtained with precise stoichiometry control. In a typical reaction, complex **1** and hexadecylamine (HDA) together with oleic acid (OlA) as ligands are dissolved in mesitylene and maintained at the desired reaction temperature for 1 h. When using the same conditions but other stabilizing systems like HDA, OlA or TOP, unstabilized materials were obtained: metallic mirrors in the first two cases and large blocks in the latter. Thus, only the combination of HDA and OlA results in the formation of nanoparticles indicating that the presence of both ligands is required, presumably for inducing a soft but robust template.[23] Examination of the influence of the ligand concentration relative to the amount of the precursor showed that the optimal ratio $[(CO)_4Fe(PH_3)]$/HDA/OlA for the synthesis of a narrow size distribution of spheres is 1/0.5/0.5. As evidenced by TEM and HRTEM, individual spherical particles of mean diameter 3.4(0.7) nm are prepared (Fig. S1, ESI†).

In order to investigate the reaction mixture in particular the carbonyl compounds were monitored during the whole procedure. It showed that the precursor transformed before decomposition to iron phosphide material. During the thermolysis in mesitylene, the color change from yellow to brown is accompanied by the appearance of new IR absorptions at 2066, 2027 and 1994 cm^{-1} (Fig. S2, ESI†). The isolation of this intermediate species was not possible using a thermolytic approach. However, irradiation of **1** yielded the same intermediate compound and allowed its isolation. The full characterization of this species led to the identification of the binuclear phosphide complex $[(CO)_3Fe(\mu\text{-}PH_2)]_2$ (**2**) (eqn (2)).

$$2[(CO)_4Fe(PH_3)] \xrightarrow[-2CO/-H_2]{h\nu/toluene} [(CO)_3Fe(\mu\text{-}PH_2)]_2 \quad (2)$$

The decomposition mechanism of **1** involves the release of CO ligands and is somewhat reminiscent to that observed for the single source precursors $Fe(SiCl_3)_2(CO)_4$ and $Co(SiCl_3)_2(CO)_4$ of the metal silicide MSi (M = Fe, Co).[24]

Interestingly, the existence of the binuclear iron complex without organic substituents at the P atoms (**2**) has already been predicted by theoretical computations.[25] However, it has not been isolated and characterized successfully to date. The highly volatile product **2** is purified by slow sublimation at normal pressure. The orange crystals so obtained are soluble in non-polar solvents such as hexane or toluene. The EI mass spectrum shows the molecular ion peak and the characteristic fragmentation pattern of successive CO elimination. The IR spectrum of **2** in KBr reveals three absorptions for the CO valence frequencies at 2071 (s), 2018 (vs) and 1995 (vs) cm^{-1}.

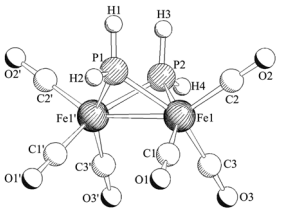

Fig. 1 Molecular structure of **2** in the crystal. Selected bond lengths (Å) and angles (°): Fe1–Fe1′ 2.635(3), Fe1–P1 2.215(9), Fe1–P2 2.220(5), Fe1–C(av) 1.806, P1–Fe1–P2 77.26(1).

Furthermore, typical absorptions at 2363 (w) and 2331 (w) cm^{-1} for the P–H valence stretching frequencies are observed. The $^{31}P\{^1H\}$ NMR spectrum exhibits a singlet at −10.1 ppm which gives a multiplet of higher order in the coupled spectrum due to the magnetically non-equivalent atoms P_A, and $P_{A'}$ as well as H_X, $H_{X'}$ and H_Y, $H_{Y'}$ atoms (see Fig. S3, ESI†). This is also reflected in the multiplet of higher order in the ^{1}H-NMR spectrum between 0.48 ppm and 3.49 ppm. The ^{1}H (Fig. S3a, ESI†) and simultaneously the ^{31}P (Fig. S3b, ESI†) NMR spectra were modeled with an AA′XX′YY′ spin system using WinDaisy[26] (Fig. S3 and Table S1, ESI†) and are in good agreement with the experimental data.

In agreement with the theoretical prediction the crystal structure of compound **2** (Fig. 1) shows a puckered Fe_2P_2 four membered ring.[27] It exhibits an angle of 78° between the two planes, which are defined by the atoms Fe1, P1, Fe1′ and Fe1, P2, Fe1′, respectively. The coordination sphere at each iron atom is completed by three terminally bound CO ligands. All bond lengths are in good agreement with the theoretically predicted ones. In particular the determined Fe–Fe distance of 2.635(4) Å is close to the calculated value of 2.619(1) Å. Analogously, the theoretical Fe–P bond length of 2.218(2) Å is between the experimental ones (2.215(9) Å and 2.220(6) Å). Even the P···P distance of 2.769(6) Å is in the range of the computed distances (2.804(2) Å), even though the computational method was limited to the Hartree–Fock method at that time.[25]

In contrast to compound **2**, analogous complexes containing organic R groups at the P atoms (*e.g.* Ph, *t*Bu, Cy)[28–30] were previously reported. The Fe–Fe bond distance in **2** is comparable to a single bond distance (*e.g.* 2.639(3) Å in $(^iPr_2NPNHPh)(^iPr_2NPH)Fe_2(CO)_6$ (ref. 31)), whereas the Fe–P bond lengths tend to be longer (*e.g.* between 2.206(4) Å and 2.246(4) Å in $(^iPr_2NPNHPh)(^iPr_2NPH)Fe_2(CO)_6$ (ref. 31)) due to the repulsion of the bulky substituents.

During the synthetic process of NPs, the binuclear complex **2** is then further converted into a molecular species showing three absorptions for the CO frequencies at 2037, 2020 and 1995 cm^{-1} in the IR spectrum (Fig. S2, ESI†). We did not succeed in isolating and identifying this cluster; however, the absence of bridging CO absorption suggests the sole formation of phosphorus-based bridging ligands. Complex **2** may, thus, be considered as the building block to yield iron phosphide material. The presence of Fe_2P_2 moieties in the unit cell of bulk FeP (MnP-type crystal structure)[1,32] also favours this assumption.

The synthesis of FeP NPs is highly reproducible and, in contrast to all previously reported routes which involve TOP and/or TOPO,[2] precise determination of the iron and phosphorus content of the as-prepared nanoparticles can be evidenced by elemental analysis. The analysis using ICP-MS indicates that our method allows precise

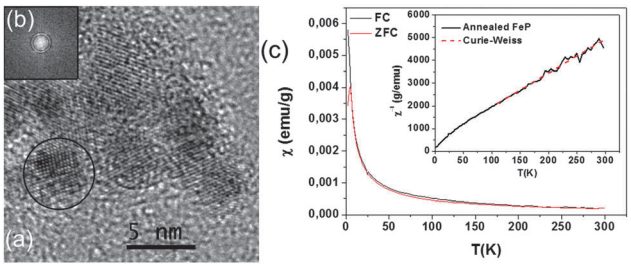

Fig. 2 HRTEM picture (a) and selected area diffraction pattern (b) of the encircled FeP nanoparticles. Temperature dependence ZFC-FC susceptibility (c).

control of Fe and P contents in a 1 : 1 ratio. XRD analysis showed amorphous FeP material, but crystalline nanoparticles displaying the orthorhombic structure of bulk FeP were obtained by annealing at 200 °C (Fig. S4, ESI†).

HRTEM analysis (with Fast Fourier Transform patterns) of single nanoparticles revealed distinct lattice fringes (Fig. 2a and b) confirming unambiguously the presence of crystalline particles. The electron diffraction pattern was taken for a small assembly of nanocrystals (~10) and ring diffractions with d values of 2.72, 2.43, 2.01 and 1.90 Å can be identified, respectively, as (011), (111), (201) and (211) peaks for the FeP orthorhombic structure (Fig. S5, ESI†).

The magnetic properties of the annealed FeP nanoparticles were measured using a superconducting quantum interference device (SQUID) in the temperature range between 2 K and 300 K. Our experimental data evidence an antiferromagnetic behaviour as expected from bulk FeP.[33] Zero-Field Cooled (ZFC) and Field Cooled (FC) measurements under an applied field of 10 Oe superimpose above 5 K, thus no evidence of ferromagnetism, due to Fe_2P impurities could be revealed. The susceptibility displays a Curie–Weiss behaviour with a θ value of 35 K. Below 110 K, the inverse susceptibility begins to deviate from the linear extrapolation. The annealed FeP nanoparticles exhibit an ordering Neel temperature of ~110 K, in agreement with T_N = 120 K measured for bulk FeP.[34] Magnetization measurements at 2 K performed according to ZFC and FC at 5 T are perfectly superimposed (Fig. S6, ESI†). They show a small coercivity ($\mu_0 H_C$ = 100 mT) and an unsaturated magnetization at 5 T and 2 K of 2.78 μB per Fe atom and in the same range as 2.98 μB reported for 5 nm FeP NPs by Perera *et al.*[34] Mössbauer spectroscopy recorded at 5 K confirms the presence of pure FeP, characterized by a doublet with an isomer shift δ = 0.4 mm s^{-1} and a quadrupolar splitting ΔEq = 0.4 mm s^{-1} (Fig. S7, ESI†). These values are in agreement with the reported values which were recorded at 293 K for bulk FeP (δ = 0.3 mm s^{-1}, ΔEq = 0.6 mm s^{-1}).[33]

In conclusion, we have presented here a low temperature route to synthesize size- and stoichiometry-controlled FeP nanoparticles. Our approach which relies on a single source precursor featuring fixed Fe : P stoichiometry, labile CO ligands and weak P–H bonds makes possible the precise control of the final material and, unprecedentedly, establishes the direct relationship between a precursor stoichiometry and the final product. Examination of the mechanism allowed the identification of intermediate clusters that are the building blocks yielding the FeP phase. This work stresses the relevant and central choice of the ligands and susbtituents to allow their removal under soft conditions while keeping intact Fe–P. Given the rich and well-known chemistry of iron carbonyl complexes incorporating phosphine ligands, this result opens up promising perspectives in the synthesis of other Fe_xP_y phases through the design of organometallic species displaying defined Fe : P ratios.

This work was supported by the Université Paul Sabatier, the CNRS and the Institut National des Sciences Appliquées of Toulouse. We thank Laure Vendier for XRD measurements, Vincent Collière for HRTEM characterization and Jean-François Meunier for SQuID and Mössbauer measurements.

Notes and references

1 S. L. Brock and K. Senevirathne, *J. Solid State Chem.*, 2008, **181**, 1552.
2 E. Muthuswamy, P. R. Kharel and S. L. Brock, *ACS Nano*, 2009, **3**, 2383.
3 Y. Xu, R. Wu, J. Zhang, Y. Shi and B. Zhang, *Chem. Commun.*, 2013, **49**, 6656.
4 S. Boyanov, J. Bernardi, F. Gillot, L. Dupont, M. Womes, J.-M. Tarascon, L. Monconduit and M.-L. Doublet, *Chem. Mater.*, 2009, **21**, 3684.
5 S. Carenco, D. Portehault, C. Boissière, N. Mézailles and C. Sanchez, *Chem. Rev.*, 2013, **113**, 7981.
6 J.-H. Chen, M.-F. Tai and K.-M. Chi, *J. Mater. Chem.*, 2004, **14**, 296.
7 C. Qian, F. Kim, L. Ma, F. Tsui, P. Yang and J. Liu, *J. Am. Chem. Soc.*, 2004, **126**, 1195.
8 J. Park, B. Koo, K. Y. Yoon, Y. Hwang, M. Kang, J.-G. Park and T. Hyeon, *J. Am. Chem. Soc.*, 2005, **127**, 8433.
9 N. Singh, P. K. Khanna and P. A. Joy, *J. Nanopart. Res.*, 2009, **11**, 491.
10 J. Park, B. Koo, Y. Hwang, C. Bae, K. An, J.-G. Park, H. M. Park and T. Hyeon, *Angew. Chem., Int. Ed.*, 2004, **43**, 2282.
11 A. E. Henkes and R. E. Schaak, *Chem. Mater.*, 2007, **19**, 4234.
12 M. Veith, *J. Chem. Soc., Dalton Trans.*, 2002, 2405.
13 M. A. Malik, M. Afzaal and P. O'Brien, *Chem. Rev.*, 2010, **110**, 4417.
14 A. C. Colson, C.-W. Chen, E. Morosan and K. H. Whitmire, *Adv. Funct. Mater.*, 2012, **22**, 1850.
15 J. P. Carpenter, C. M. Lukehart, S. B. Milne, S. R. Stock, J. E. Wittig, B. D. Jones, R. Glosser and J. G. Zhu, *J. Organomet. Chem.*, 1998, **557**, 121.
16 A. T. Kelly, I. Rusakova, T. Ould-Ely, C. Hofman, A. Lüttge and K. H. Whitmire, *Nano Lett.*, 2007, **7**, 2920.
17 E. O. Fischer, E. Louis and J. Mueller, *Chem. Ber.*, 1969, **102**, 2547.
18 H. Schäfer and W. Z. Leske, *Z. Anorg. Allg. Chem.*, 1987, **552**, 50.
19 D. L. Huber, *Small*, 2005, **1**, 482.
20 A. C. Colson and K. H. Whitmire, *Chem. Mater.*, 2011, **23**, 3731.
21 M. Scheer, U. Vogel, U. Becker, G. Balazs, P. Scheer, W. Hönle, M. Becker and M. Jansen, *Eur. J. Inorg. Chem.*, 2005, 135.
22 C. Dreher, M. Zabel and M. Scheer, *Organometallics*, 2010, **29**, 5187.
23 L.-M. Lacroix, S. Lachaize, A. Falqui, M. Respaud and B. Chaudret, *J. Am. Chem. Soc.*, 2009, **131**, 549.
24 A. Zhao, X. Chen, J. Guan, C. T. Williams and C. Liang, *Phys. Chem. Chem. Phys.*, 2011, **13**, 9432; C. Liang, A. Zhao, X. Ma, Z. Zhang and R. Prins, *Chem. Commun.*, 2009, 2047; J. Guan, A. Zhao, X. Chen, M. Zhang and C. Liang, *Stud. Surf. Sci. Catal.*, 2010, **175**, 259.
25 M. B. Hall, R. F. Fenske and L. F. Dahl, *Inorg. Chem.*, 1975, **14**, 3103.
26 *WinDaisy, Version 4. 05*, Bruker-Franzen Analytik GmbH.
27 $C_6H_4Fe_2O_6P_2$, M = 345. 73, monoclinic, space group $P2_1/m$ (no. 11), a = 6.2476(7) Å, b = 12.9819(11) Å, c = 7.2193(8) Å, β = 90.135(14)°, V = 585.53(10) Å^3, Z = 2, μ = 2.755 mm^{-1}, $F(000)$ = 340, T = 123(1) K, 8337 reflections measured, 1444 unique (R_{int} = 0.0131), R_1 = 0.0258, wR_2 = 0.0751 for $I > 2\sigma(I)$. CCDC 818354.
28 P. M. Treichel and W. M. Douglas, *J. Organomet. Chem.*, 1972, **42**, 145.
29 B. Walther, H. Hartung, J. Reinhold, P. G. Jones, H.-C. Bottcher, U. Baumeister and A. Krug, *Chem. Ber.*, 1992, **125**, 1379–1382.
30 V. Kumar, D. W. Lee and R. B. King, *J. Organomet. Chem.*, 1996, **512**, 1.
31 L. Hirsivaara and J. Pursiainen, *Eur. J. Inorg. Chem.*, 2001, 2255.
32 A. P. Governor, S. D. Wik and A. Mar, *Inorg. Chem.*, 2005, **44**, 8988.
33 S. Boyanov, L. Monconduit and D. Zitoun, *Chem. Mater.*, 2009, **21**, 3684.
34 S. C. Perera, P. S. Fodor, G. M. Tsoi, L. E. Wenger and S. L. Brock, *Chem. Mater.*, 2003, **15**, 4034.

